Brain Imaging and Behavior
https://doi.org/10.1007/s11682-020-00316-4

ORIGINAL RESEARCH

Endocytosis-pathway polygenic scores affects the hippocampal network connectivity and individualized identification across the high-risk of Alzheimer's disease

Yao Zhu[1] · Feifei Zang[1] · Xinyi Liu[1] · Dandan Fan[1] · Qianqian Zhang[1] · Qingguo Ren[1] · Chunming Xie[1] · for the Alzheimer's Disease Neuroimaging Initiative

Abstract

The neural mechanisms underlying the polygenic effects of the endocytosis pathway on the brain function of Alzheimer's Disease (AD) remain unclear, especially in the prodromal stages of AD from early mild cognitive impairment (EMCI) to late mild cognitive impairment (LMCI). We used an imaging genetic approach to investigate the polygenic effects of the endocytosis pathway on the hippocampal network across the prodromal stages of AD. The subjects' data were selected from the Alzheimer's Disease Neuroimaging Initiative. Hippocampal volumes were examined in subjects of cognitive normal (CN), EMCI and LMCI groups. Multivariate linear regression analysis was employed to measure the effects of disease and endocytosis-based multilocus genetic risk scores (MGRS) on the hippocampal network which was constructed using the bilateral hippocampal regions. We identified hippocampal volumes in LMCI group were smaller than those in CN and EMCI groups. Endocytosis-based MGRS was widely influenced the neural structures within the hippocampal network, especially in the prefrontal-occipital regions and striatum. Compared to low endocytosis-based MGRS carriers, high MGRS carriers showed the opposite trajectory of hippocampal network functional connectivity (FC) across the prodromal stages of AD. Further, a model composed of selected hippocampal FCs and hippocampal volume yielded strong classification powers of EMCI and LMCI. These findings expand our understanding of the pathophysiology of polygenic effects underlying brain network in the prodromal stages of AD.

Keywords Genetic polymorphism · Mild cognitive impairment · Hippocampus · Resting-state functional magnetic resonance imaging · Classification

Introduction

Alzheimer's disease (AD) is a neurodegenerative disease featured by severe cognitive impairment in the elderly. The incidence of AD has been on the rise, but unfortunately, to date we have not found a complete cure for AD (2016 Alzheimer's disease facts and Figs. 2016). The National Institute on Aging-Alzheimer's Association (NIA-AA) research framework defines AD as a biological process that spans from normal to dementia (Cummings 2018). Pathological changes may begin decades before the onset of dementia and substantial neuronal loss in the prodromal stages of the AD (Atri 2019; Sperling et al. 2011). Therefore, Healthy lifestyle and preventive treatment are encouraged in the prodromal stages of dementia and reducing dementia risk factors may slow the progression of AD (Smith and Yaffe 2014; Sperling et al. 2014). The intermediate stage between cognitively normal and dementia is mild cognitive impairment (MCI). Therefore, more and more people are concerned about the decline of cognitive ability in MCI patients (Mitchell 2009; Koivunen et al. 2011). The Alzheimer's Disease Neuroimaging Initiative (ADNI) split

Electronic supplementary material The online version of this article (https://doi.org/10.1007/s11682-020-00316-4) contains supplementary material, which is available to authorized users.

✉ Qingguo Ren
101011331@seu.edu.cn

✉ Chunming Xie
101011769@seu.edu.cn

[1] Department of Neurology, School of Medicine, Affiliated ZhongDa Hospital, Southeast University, Nanjing 210000, Jiangsu, China

Published online: 16 August 2020

MCI stage into two phases—early MCI (EMCI) and late MCI (LMCI)—according to the severity of delayed memory impairment in logical memory (Aisen et al. 2010; Weiner et al. 2010). Understanding the differences between EMCI and LMCI may help to understand AD progression.

The pathological marker of AD is β-amyloid protein (Aβ) (Hardy and Selkoe 2002; Musiek and Holtzman 2015). Increasing evidence have reported that endocytosis takes effect in the Aβ metabolism (Cirrito et al. 2008; Choy et al. 2012; Carey et al. 2005). Endocytosis is the active transport system that involves the cell membrane in trafficking molecules move in and out of the cell through endocytic transport system across the membrane, and all components of this system make up endocytic pathway. Endocytosis occurs when partial entrapment of plasma membrane, in which the contents of vesicle are internalized by clathrin-dependent or clathrin-independent pathways (Miaczynska et al. 2004; Sorkin and Von Zastrow 2002; Hansen and Nichols 2009). Neurons can clear β-amyloid precursor protein (APP) by endocytosis pathway. Genetic studies have shown that the onset and progression of AD are associated with some endocytosis-related genes (Seshadri et al. 2010; Harold et al. 2009; Hollingworth et al. 2011; Naj et al. 2011; Lambert et al. 2013). Therefore, mutations in endocytic genes that disrupt physiological functions of neurons might significantly contribute to AD pathophysiology (Kimura and Yanagisawa 2018). *BIN1* gene encodes for bridging integrator 1(BIN1), via interaction of clathrin and the AP-2/α-adaptin (CLAP) domain, regulates the endocytosis pathway(Ramjaun and McPherson 1998). BIN1 increases Aβ by binding to GTPase dynamin via clathrin-mediated endocytosis (Wigge and McMahon 1998). Recent evidence suggests that BACE1 is modulated by *BIN1*, then adjusting the Aβ production (Miyagawa et al. 2016; Ubelmann et al. 2017). *CD2AP* gene encodes CD2-associated protein which(CD2AP) is a membrane-associated scaffold protein involved in intracellular trafficking (Dustin et al. 1998), a key regulator of lysosome vesicle transport (Cormont et al. 2003) and a major candidate for regulating Aβ clearance. *SORL1* gene encodes for sortilin related receptor 1(SORL1). It is responsible for the transport of vesicles from the cell surface to the golgi endoplasmic reticulum and binds directly to APP for recycling and contribute to the Aβ generation (Lee et al. 2008; Spoelgen et al. 2006; Schmidt et al. 2007). SORL1 is also a receptor that binds lipoproteins, with a preference for apolipoprotein E ε4 (*APOE* ε4)—high risk gene for AD, and mediates the cellular uptake via endocytic pathway(Rogaeva et al. 2007; Yajima et al. 2015). *PICALM* gene encodes for phosphatidylinositol binding cathrin assembly protein(PICALM) which is also commonly seen in neurons(Xiao et al. 2012). Generally, this protein is involved in the clathrin assembly, regulation of endocytosis and cell transport (Baig et al. 2010), and also associated with cell proliferation and iron homeostasis (Scotland et al. 2012). In addition, PICALM plays an important role in the fusion of synaptic vesicles and presynaptic membranes through the transport of synaptic vesicle-related membrane proteins (Harel et al. 2008). Studies on the correlation among *PICALM* variants, cognitive function, and assessment of brain volume, have shown that *PICALM* variation has a protective effect (Mengel-From et al. 2011; Biffi et al. 2010).

The hippocampus was core structure of the episodic memory network and those with smaller volumes represent the most important structural hallmark of conversion from MCI to AD (Bai et al. 2009b; Dickerson et al. 2001; Bottino et al. 2002; Pennanen et al. 2004). Resting-state functional magnetic resonance imaging (rs-fMRI) studies have also found the alteration of hippocampal functional connectivity (HFC) network across the AD spectrum (Sohn et al. 2014; Wang et al. 2006). Decreased FC in hippocampal subregion was associated with episodic memory declines with amnestic mild cognitive impairment(aMCI) (Bai et al. 2011). Ye et al. found that *APOE* genotype could affect the aging trajectories of compensation in the HFC network in aMCI subjects (Ye et al. 2016). However, the occurrence of AD may ascribe to the summative effects of multiple genes related to the onset and development of AD (Liu et al. 2012; Williamson et al. 2009). Our group has previously reported that tau protein pathway and insulin resistance pathway genes played significant roles in the pathology of MCI with rs-fMRI studies (Bai et al. 2016; Su et al. 2017a). Recently, a study by constructing multiple genetic risk scores (MGRS) to investigated their association with AD, MCI, and brain magnetic resonance structural phenotypes, implying that the MGRS capturing endocytosis pathway was significantly associated with MCI (Ahmad et al. 2018). However, multiple genes effects of the endocytic pathway on the brain function appear to be unknown in the AD spectrum.

The purpose of this study was to explore the neural mechanism of multiple genetic effect of the endocytic pathway on the HFC network in the EMCI and LMCI patients. We hypothesized that HFC network would be significantly associated with endocytosis-based MGRS in the AD spectrum. Altered connectivities within the HFC network combining with hippocampal volumes could be used to distinguish EMCI from LMCI patients, thus, the neuroimaging biomarker for the early differentiation of prodromal stages of AD was obtained.

Material and methods

ADNI database and participants

All data were obtained from the ADNI database (http://adni.loni.usc.edu). The rs-fMRI scans images were enrolment from ADNI-1, ADNI-GO and ADNI-2 at baseline. A total of 86 subjects were enrolled in the current study, including 35

cognitive normal (CN), 32 EMCI, and 19 LMCI. Individuals with one or more *APOE* ε4 alleles were classified as *APOE* ε4 carriers (*APOE* ε4+), while subjects with no *APOE* ε4 alleles were classified as *APOE* ε4 non-carriers (*APOE* ε4-). According to the ADNI protocol, the CN subjects were verified as free of memory complaints, beyond what one would expect for age. EMCI and LMCI subjects had a subjective memory concern as reported by the subject, study partner or clinician. The EMCI and LMCI subjects' Mini-Mental State Examination (MMSE) scores were between 24 and 30, CDR scores of 0.5. To distinguish between EMCI and LMCI, abnormal memory function was documented by scoring the Logical Memory II subscale (Delayed Paragraph Recall) from the Wechsler Memory Scale-Revised after the education adjusted ranges: EMCI: (a) 9–11 for 16 or more years of education; (b) 5–9 for 8–15 years of education; (c) 3–6 for 0–7 years of education; LMCI: (a) ≤ 8 for 16 or more years of education; (b) ≤ 4 for 8–15 years of education; (c) ≤ 2 for 0–7 years of education. The functional brain MRI data and corresponding clinical data were downloaded before November 24, 2017 from the publicly available ADNI database. All the detailed description of the neuropsychological measure was presented in the Supplementary Material.

Gene selection and construction of multilocus genetic risk scores

MGRS employed in this study captures genetic variation in endocytosis from the genome-wide association studies (GWASs), including *BIN1*(rs744373), *CD2AP*(rs9296559), *PICALM*(rs3851179) and *SORL1*(rs2070045). The genome-wide single nucleotide polymorphisms (SNPs) were genotyped using the Illumina Human610-Quad Bead chip. The detailed genotyping process was described in previous study (Potkin et al. 2009). Each of the four reported SNPs has reached the threshold of $P < 5 \times 10^{-8}$ in previous GWAS (Ahmad et al. 2018; Harold et al. 2009; Hollingworth et al. 2011; Lambert et al. 2013). We used PLINK v1.08 (Purcell et al. 2007) to conduct the genetic analyses. SNPs were included as follows: minor allele frequencies (MAF) > 0.05, Hardy-Weinberg equilibrium test $P > 0.001$, minimum call rates >90%. Each SNP was tested for association with MCI in an additive model by multivariable logistic regression analysis. The genotypes were coded in the additive model as "0" for non-risk allele homozygotes, "1" for heterozygotes, and "2" for risk allele homozygotes. The significance level was set at $P < 0.05$ after FDR correction. Consequently, the four SNPs showed statistical significance and entered into weighted multilocus genetic risk scores (MGRS) calculation. The weight used for each SNP was the natural log of the odds ratio (OR) associated with the risk allele, as opposed the OR associated with the minor(sometimes protective) allele that was obtained from the meta-analysis (Lambert et al. 2013; Bertram et al. 2007). The specific information were rs744373 (Chr: 2, Postion: 127894615, risk: G, OR: 1.17, weight: 0.16), rs9296559 (Chr: 6, Position: 47484534, risk: C, OR: 1.11, weight: 0.10), rs3851179 (Chr: 11, Position: 85868640, protection: A, OR: 0.88, weight: −0.13), rs2070045 (Chr: 11, Position: 121448090, risk: G, OR: 1.06, weight: 0.06). The weighted MGRS was calculated by multiplying the number (0/1/2) of risk alleles by the weight, and subsequently obtaining the sum across the four SNPs. This detailed method has been described in previous studies (Rodriguez-Rodriguez et al. 2013; Su et al. 2017b). Moreover, since genetic neuroimaging data has identified *APOE* ε4 as a risk allele in AD and showed abnormal resting-state brain function in patients with this allele (Rodriguez-Rodriguez et al. 2013), this study included *APOE* ε4 as covariates in the following analysis.

Data acquisition

All subjects were scanned on a 3.0-Tesla Philips MRI scanner. Rs-fMRI images were obtained using an echo-planar imaging sequence with the following parameters: 140 time points, repetition time (TR) = 3000 ms, echo time (TE) = 30 ms, flip angle = 80°, number of slices = 48, slice thickness = 3.3 mm, spatial resolution = 3 × 3 × 3 mm^3, acquisition matrix = 64 × 64, and field of view (FOV) = 240 × 240 mm. All original image files were available to the general scientific community. T1-weighted images were acquired using a sagittal magnetization prepared rapid gradient echo (MP-RAGE), with data parameters: TR = 6700 ms, TE = 3.1 ms, slice thickness = 1.2 mm, FA = 9°, FOV = 250 × 250 mm, thickness = 1.0 mm, gap = 0 mm, and number of slices = 170.

Data preprocessing

The data preprocessing was performed using the Data Processing Assistant for a Resting-State fMRI (DPARSFA) (http://www.restfmri.net), which is based on Statistical Parametric Mapping (SPM12, http://www.fil.ion.ucl.ac.uk/spm) and the rs-fMRI Data Analysis Toolkit (REST, http://www.restfmri.net). Data analyses of the groups were conducted with the SPM12 toolkit. Briefly, the first 10 volumes of the scanning session were discarded to allow for T1 equilibration effects. The remaining images were corrected for timing differences and motion effects. No translation or rotation parameters of head motion in any given data set exceeded ±3 mm or ± 3°. The resulting images were spatially normalized to the standard Montreal Neurological Institute (MNI) echo-planar imaging template using the default settings, resampling to 3 × 3 × 3 mm^3 voxels, and smoothed with a Gaussian kernel of 6 × 6 × 6 mm. To further reduce the effects of confounding factors, the Friston's 24 head motion parameters, as well as white matter (WM) signal, and cerebrospinal

fluid (CSF) signal, were regressed out. Finally, a bandpass filter was applied to keep only low-frequency fluctuations between 0.01–0.08 Hz.

Voxel-wised hippocampal functional connectivity analysis

To create seeds for the connectivity analysis, bilateral hippocampal regions were separately defined using the automated anatomical labelling implemented with WFU_PickAtlas software (Maldjian et al. 2003). The defined seed regions were then resampled to the same space as the functional data. For each subject, the averaged time series of the seed region was computed as the reference time course. Then, a Pearson cross-correlation analysis was performed between the seed time course and the time course of the all brain voxels. Fisher's z-transformation was applied to improve the normality of the correlation coefficients [m = 0. 5ln(1 + r)/(1 − r)]. In this way, individual HFC network maps were obtained.

Structural image analysis and hippocampal volume assessment

The gray matter volume(GMV) was considered as an covariate in the functional connectivity analysis (Xie et al. 2011; Xie et al. 2015). An optimized voxel-based morphometry (VBM) analysis was conducted using SPM12 to calculate the GMV in all subjects. In brief, the structural images were normalized to the Montreal Neurological Institute (MNI) template using an affine and nonlinear spatial normalization. The normalized images were segmented into gray matter, white matter and cerebrospinal fluid according to MNI prior probability maps. Then, Jacobian modulation was applied to the segmented gray matter image, which can be incorporated to compensate for the effect of spatial normalization. Finally, the extracted gray matter set was smoothed with 8-mm full width at half maximum Gaussian kernel. The final images were regressed out as covariate of no interest when calculating functional connectivity. Next, the hippocampal regions were interpolated to the same dimension, sizes, and origins with individual images. A mean volume index of all of the voxels of the hippocampal region was computed for each subject. The hippocampal volume was obtained by multiplying the mean volume index by the number of voxels and the size of each voxel (Bai et al. 2009a; Ye et al. 2017).

Statistical analysis

Demographic information and neuropsychological performance

Analysis of variance (ANOVA) and chi-square tests (for gender and *APOE* ε4 status) were used to compare the demographic data. Mixed analysis of covariance (ANCOVA), with the disease and MGRS as fixed factors, was used to analyse the neuropsychological performances among subjects with statistically significant differences ($p < 0.05$) after controlling for age, gender, and education, followed by post-hoc test to determine the significance of the specific comparisons ($p < 0.05/3 = 0.017$, Bonferroni correction). All statistical procedures utilized SPSS 25.0 software.

Behavioural significance

Partial correlation analysis was performed to detect the relationship between MGRS (also individual variants) and cognitive behaviour in MCI groups after controlling for covariates including gender, age, education, and GM volumes. The significance level was set at $P < 0.05$, and the multiple comparison correction was conducted using Bonferroni adjustment. All statistical procedures utilized SPSS 25.0 software.

Group-level intrinsic HFC network analysis

To analyse the main effect and interaction of the endocytosis pathway-based MGRS and disease status on the HFC network. Multivariate linear regression analysis was employed to investigate the potential effects of disease (D), MGRS, and D × MGPS on the HFC network (3dRegAna, AFNI), after controlling for covariates including gender, age, education, and GM volumes and *APOE* ε4 status. The thresholds were set at $p < 0.01$ (cluster size ≥42 voxels) which was determined by Monte Carlo simulation for multiple comparisons after being corrected with the latest 3dClustSim program(https://afni.nimh.nih.gov/pub/dist/doc/program_help/3dClustSim.htm). The following equation is the multivariate regression analysis for identifying the neural correlates of disease, MGRS, and interaction of disease and MGRS (D × MGPS) among all subjects:

$$\begin{aligned} m_i = {} & \beta 0 + \beta 1 \times D + \beta 2 \times MGRS + \beta 3 \times (D \times MGRS) \\ & + \beta 4 \times Age + \beta 5 \times Gender + \beta 6 \times Edu + \beta 7 \\ & \times GM + \beta 8 \times APOE\varepsilon 4 + \varepsilon \end{aligned}$$

where m_i is the m value of the *i*th voxel across all subjects, β0 is the intercept of the straight line fitting in the model, and β1, β2, β3 are the main effects of disease, MGRS and D × MGRS. β4, β5, β6, β7 and β8 are the effects of age, gender, education, gray matter atrophy, and *APOE* ε4 status, respectively, as covariates of no interest in the linear regression model. All results were projected onto the surface brain template. To quantitatively represent these altered HFC strength, the averaged m-values (correlation coefficients after Fisher z transformation) in each target region of interest (ROI) was extracted from the individual HFC network and shown with histograms using the rs-fMRI Data Analysis Toolkit (REST) 1.8.

The relative variance of the HFC network was calculated, which can be explained by the endocytosis-based MGRS. The extracted average FC strength in each ROI from the main effect of endocytosis-based MGRS on HFC network was selected and entered into linear and stepwise regression models after controlling for the effects of age, gender, education, gray matter atrophy, and *APOE* ε4 status.

Exploratory classification analysis

We tested the neuroimaging measures of brain regions with significant difference among the groups as candidate variables, including the altered regional FC strengths and hippocampal volumes, to see if they could be used as distinguishing features between EMCI and LMCI patients, as previously described in publications (Ranasinghe et al. 2014; Weiler et al. 2014). Neuroimaging indices of each subject in the EMCI and LMCI groups were used as features and then entered into the stepwise discrimination analysis. To test the robustness of the results, the leave-one-out cross-validation method was used. The predictive value was estimated with receiver operating characteristic (ROC) curves by calculating the sensitivity, specificity, and area under the curve (AUC). Unless specifically mentioned, the threshold for statistical significance was defined as $p < 0.05$.

Results

Demographic information and neuropsychological data

As shown in Table 1, no significant differences were found in age, gender, *APOE* ε4 status, education, GMV or MGRS among all the participants (all $p > 0.05$). Compared with CN group, EMCI group displayed significant impairment in cognitive behavior as assessed by the ADAS-cog and RAVLT-immediate recall. Compared with CN and EMCI groups, LMCI group displayed poorer performance on the ADAS-cog and RAVLT (except forgetting). Further, each group subjects were divided into two subgroups according to the method described in the previous study (Xu et al. 2018). Subjects with MGRS ≥ 0.11 (averaged MGRS of all subjects = 0.11) were defined as the high endocytosis-based MGRS subgroup while the others were low endocytosis-based MGRS subgroup. There were no significant differences in allele frequency in the four gene loci among the three groups (Table S1).

Hippocampal volume

The mean volume index of the hippocampal region in each group was calculated by interpolating the hippocampus to the individual gray matter images segmented from the T1 images (Fig. 2a). As presented in Fig. 2b, the volumes of the left or right hippocampus in LMCI group were significantly smaller than those in CN and EMCI groups (left, 3690.65 ± 441.51 mm^3 in LMCI group vs. 3968.98 ± 398.31 mm^3 in CN group and 3971.13 ± 393.06 mm^3 in EMCI group, both $p < 0.05$; right, 3633.47 ± 467.92 mm^3 in LMCI group vs. 3876.70 ± 373.57 mm^3 in CN group and 3882.96 ± 326.03 mm^3 in EMCI group, both $p < 0.05$). As expected, the LMCI group had declining bilateral total hippocampal volumes compared with the CN and EMCI groups (7324.12 ± 824.78 mm^3 in LMCI group vs. 7845.67 ± 751.65 mm^3 in CN group and 7854.09 ± 691.04 mm^3 in EMCI group, both $p < 0.05$).

Main effects of the endocytosis-based MGRS and disease status on the HFC network

Endocytosis-based MGRS was associated with both positive and negative effects on the HFC network (Fig. 2). Specifically, the positively correlated regions were primarily located in the right fusiform area (RFFA) and left orbitofrontal cortex (LOFC) on the left HFC network, and also the RFFA was found on the right HFC network. While the negatively correlated regions included the bilateral cuneus (BCUN) on the left and right HFC network. Moreover, the linear regression models revealed that the endocytosis-based MGRS accounted for 5.8–11.4% of all variability in ROIs on the HFC network. These contributions were significant in BCUN ($R^2 = 0.064$, $\beta = -0.272$, $p = 0.009$), RFFA ($R^2 = 0.114$, $\beta = -0.230$, $p = 0.024$) on the left HFC network and BCUN ($R^2 = 0.058$, $\beta = -0.261$, $p = 0.012$) on the right HFC network.

Compared with CN group, EMCI and LMCI groups showed gradually increased positive connectivity within the HFC network (Fig. 3), including bilateral nucleus accumbens (BNAcc) and right posterior middle temporal gyrus (RpMTG) on the left HFC network and bilateral thalamus (BTHA) on the right HFC network. Brain region with decreased negative connectivity was mainly in the right inferior parietal cortex/right temporal-parietal junction (RIPC/RTPJ) on the left HFC network.

Interactive effects between endocytosis-based MGRS and disease status on HFC network

Significant interactions of endocytosis-based MGRS and disease status on the HFC network were identified. These regions were seen in frontal-temporal-occipital-striatum system, including the bilateral caudate (BCAU), BCUN, BNAcc, LOFC and RFFA on the left HFC network, the RCUN and RFFA on the right HFC network. In order to reveal the specific interactive pattern of endocytosis-based MGRS and disease in HFC network, we divided all subjects into high MGRS (36 subjects, MGRS ≥ 0.11) and low MGRS subgroups (50

Table 1 Demographic information and neuropsychological data

	CN	EMCI	LMCI	F/X^2	*P* value
Age	73.81 ± 4.87	71.33 ± 7.57	72.39 ± 6.64	1.28	0.284
Gender(M/F)	16/19	11/21	12/7	3.99	0.136
APOE (ε4±)	11/24	17/15	9/10	3.40	0.183
Education	16.11 ± 2.35	15.25 ± 2.82	16.21 ± 2.88	1.16	0.318
GMV (ml)	573.56 ± 46.87	578.78 ± 55.27	556.90 ± 47.77	1.16	0.318
MMSE	28.66 ± 1.35	28.48 ± 1.56	27.87 ± 1.46	2.13	0.125
CDR-SB	1.60 ± 0.50	1.58 ± 0.50	1.57 ± 0.51	0.04	0.963
ADAS-cog	9.69 ± 3.62	12.48 ± 5.92	16.93 ± 5.39	14.53	<0.001 [abc]
RAVLT					
Sum	37.49 ± 21.81	48.85 ± 29.22	65.62 ± 24.22	8.57	<0.001 [bc]
Immediate	43.80 ± 9.30	39.09 ± 10.09	33.30 ± 6.41	9.51	<0.001 [abc]
Learning	5.94 ± 2.39	5.76 ± 2.67	3.39 ± 2.21	8.65	<0.001 [bc]
Forgetting	3.94 ± 2.34	4.45 ± 2.44	5.30 ± 2.08	2.41	0.096
MGRS	0.10 ± 0.15	0.13 ± 0.15	0.08 ± 0.17	0.64	0.530
MGRS (high/low)	15/20	12/20	9/10	0.50	0.778

χ^2 test was applied in the comparisons of gender, APOE genotype and MGRS status, and one-way ANOVA was applied in the other comparisons. High MGRS ≥0.11; Low MGRS<0.11. Significant differences ($p < 0.05$) were found in ADAS-cog and RAVLT (except for forgetting) among three groups

a–c: post-hoc analysis further revealed the source of ANOVA difference (a: EMCI vs CN; b: LMCI vs CN; c: EMCI vs LMCI)

CN cognitive normal, *EMCI* early mild cognitive impairment, *LMCI* late mild cognitive impairment, *F/M* female/male, *GMV* gray matter volume, *ml* milliliter, *MMSE* mini-mental state examination, *ADAS-Cog* 13-item Alzheimer's Disease Assessment Scale-Cognitive subscale, *RAVLT* Rey auditory verbal learning test, *MGRS* multilocus genetic risk scores

subjects, MGRS <0.11). Compared with low endocytosis-based MGRS carriers, the high endocytosis-based MGRS carriers showed approximately opposite trajectory changes in the HFC network across the prodromal stages of AD, especially in the CN and EMCI stages. Specifically, the high endocytosis-based MGRS carriers represented increased connectivity in the BCAU and BCUN from the CN to LMCI, as well as decreased connectivity in the LOFC, BNAcc, and RFFA, while the low endocytosis-based MGRS carriers showed a completely inverted mode, as displayed in Fig. 4.

Behavioral significance in MCI groups

Partial correlation analysis revealed that the risk score of *SORL1* was positively correlated with RAVLT-immediate ($r = 0.28$, $p = 0.049$) in MCI groups (include EMCI and

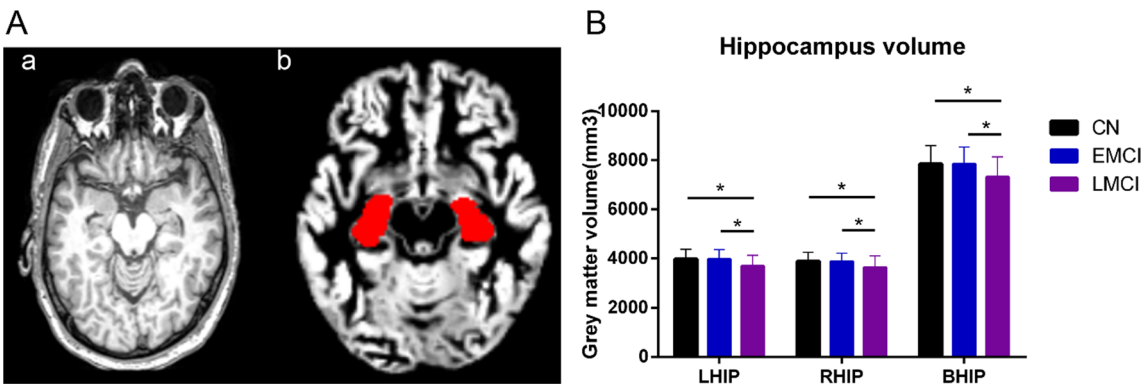

Fig. 1 **a** Hippocampal volume assessment. (*a*) The grey matter was segmented from T1 images. (*b*) The left/right side hippocampus, isolated using automated anatomical labeling, was interpolated to individual gray matter images. A mean volume index of all voxels of the hippocampal regions was computed for each subject. **b** The two sides and total hippocampal volumes. The LMCI subjects had smaller hippocampal volumes than the control and EMCI subjects. Abbreviation: *CN* cognitive normal, *EMCI* early mild cognitive impairment, *LMCI* late mild cognitive impairment, *LHIP* left hippocampus, *RHIP* right hippocampus, *BHIP* bilateral hippocampus

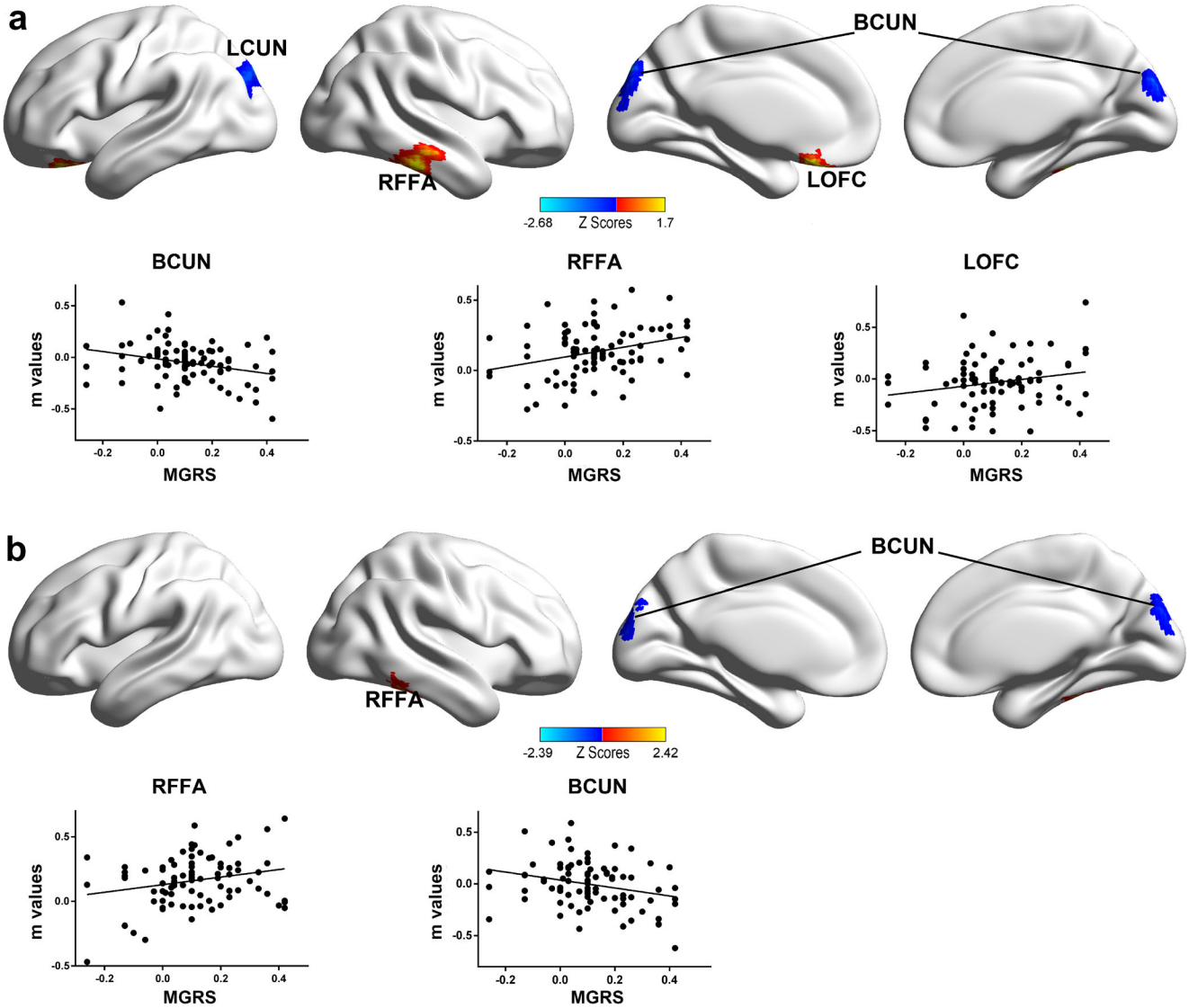

Fig. 2 Main effects of endocytosis-based MGRS on the HFC network across all subjects. Brain regions significantly affected by endocytosis-based MGRS in bilateral HFC networks were shown in (**a**) (left HFC network) and (**b**) (right HFC network). Bright color indicated a positive correlation between the endocytosis-based MGRS and HFC network among all subjects, while blue color indicated a negative correlation. Numerical representations of positive and negative correlations between endocytosis-based MGRS and HFC strength among all subjects were plotted. (m is z value from the cross-correlation coefficient after Fisher's z transformed, same below). Abbreviation: *MGRS* multilocus genetic risk scores, *HFC* hippocampal functional connectivity, *LCUN* left cuneus, *BCUN* bilateral cuneus, *LOFC* left orbitofrontal cortex, *RFFA* right fusiform area

LMCI groups), but this correlation was not significant after Bonferroni correction. We did not find any other significant correlations between individual endocytosis variants and the cognitive behavioral scores, or between endocytosis-based MGRS and cognitive behavioral scores (all $p > 0.05$, **Table S2**).

Exploratory classification analysis

We selected neuroimaging measures as independent variables for classification biomarker using a Fisher linear stepwise discriminate analysis. In the high endocytosis-based MGRS carriers, with the LHIP-RpMTG FC and LHIP volume as discriminative features, the model achieved the accuracy of 81.0% to distinguish the EMCI from the LMCI patients (sensitivity, 83.3%; specificity, 77.8%) and an AUC = 0.833. While in the low endocytosis-based MGRS carriers, taking the LHIP-RTPJ, LHIP-RpMTG, RHIP-BCUN, and RHIP-RFFA FCs as discriminative features, the model achieved the accuracy of 83.3% (sensitivity, 85.0%; specificity, 80.0%) and an AUC = 0.965. Besides, the leave-one out cross-validation results showed the accuracy of 76.2% and 76.7% respectively, indicating relatively high diagnostic power (Table S3–4, Fig. 5). Regardless of the endocytosis-based

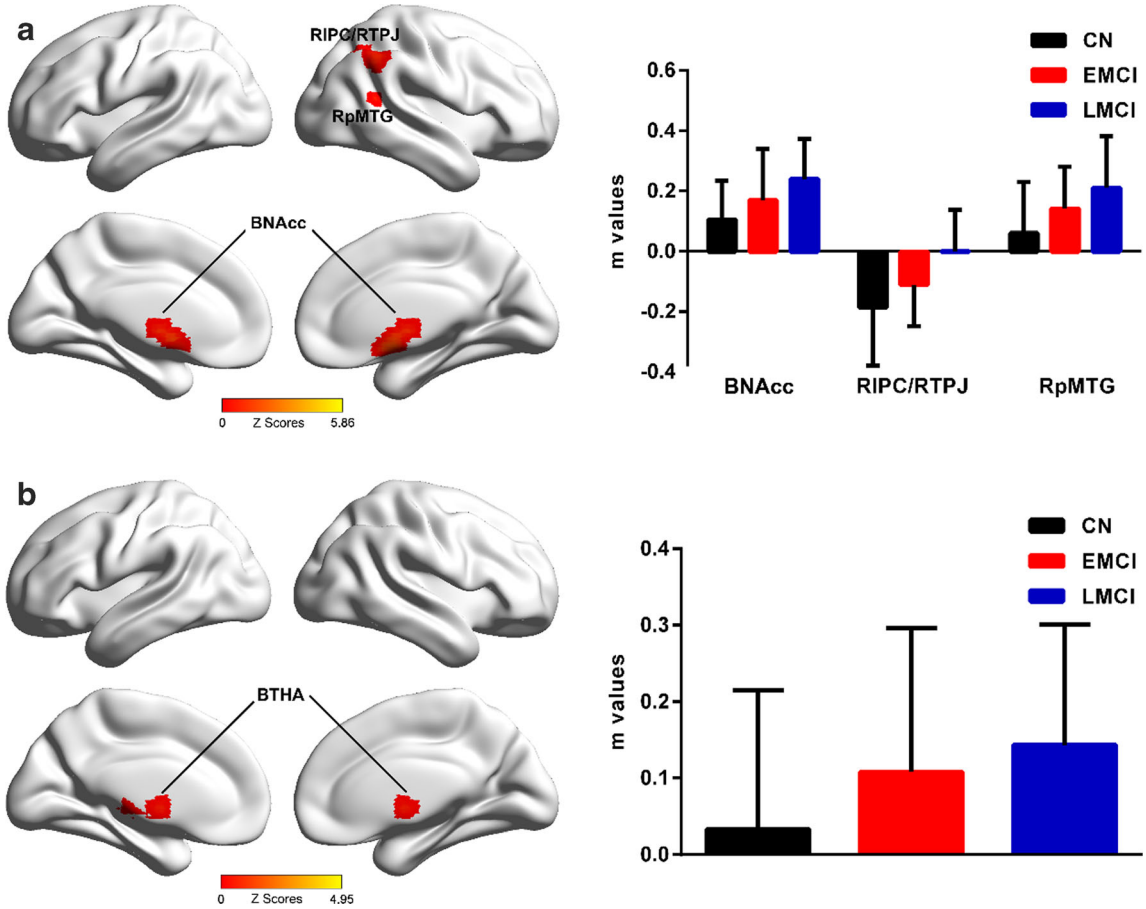

Fig. 3 Main effects of disease status on the HFC network across all subjects. Brain regions significantly affected by disease in bilateral HFC networks were shown in (**a**) (left HFC network) and (**b**) (right HFC network). The numerical representations of main effects of disease status on the HFC among all the groups were illustrated with bar charts. RIPC/RTPJ indicated gradually decreased FC but other regions showed increased FC towards a CN trend in the LMCI stage. Abbreviation: *CN* cognitive normal, *EMCI* early mild cognitive impairment, *LMCI* late mild cognitive impairment, *HFC* hippocampal functional connectivity, *BNAcc* bilateral nucleus accumbens, *RIPC/RTPJ* right inferior parietal cortex/ right temporal-parietal junction, *RpMTG* right posterior middle temporal gyrus, *BTHA* bilateral thalamus

MGRS status, the most discriminative features for classification included the bilateral hippocampus volumes and LHIP-RIPC/RTPJ FC. This classification model achieved the accuracy of 76.5% between the two groups (sensitivity, 81.3%; specificity, 68.4%) and an AUC = 0.766 (Table S5, Fig. S1). The cross-validation results also showed that 72.5% of subjects in both groups could be correctly classified.

Discussion

In this study, we demonstrated the cumulative effects of multiple gene polymorphisms in the endocytosis pathway on the HFC network in MCI patients and the divergent trajectory of the HFC network pattern in the high endocytosis-based MGRS carriers compared to the low endocytosis-based MGRS carriers across the prodromal stages of AD. Endocytosis-based MGRS influenced the HFC network and accounted for 5.8–11.4% of all variability of the HFC network. More importantly, studies on prodromal AD suggested that the hippocampus atrophy was more obvious in MCI patients than that of elderly (Jessen et al. 2010; Zhao et al. 2019). In our study, we found that only hippocampal volumes of LMCI patients were smaller than that of EMCI patients and control subjects, while there was no such difference between EMCI patients and control subjects. Furthermore, we also determined that these altered FCs and hippocampal volumes could classify the population in prodromal stages of AD with good sensitivity and specificity and represent a potential neuroimaging biomarker in the disease stage-dependent manner. Previous study found endocytosis genetic risk scores associated with MCI and AD (Ahmad et al. 2018). It is not clear whether multiple genes in the endocytosis pathway are involved in the disengagement of HFC network. The present study provided direct evidence that the endocytosis genetic profile differentially influenced HFC network across the prodromal stages of AD.

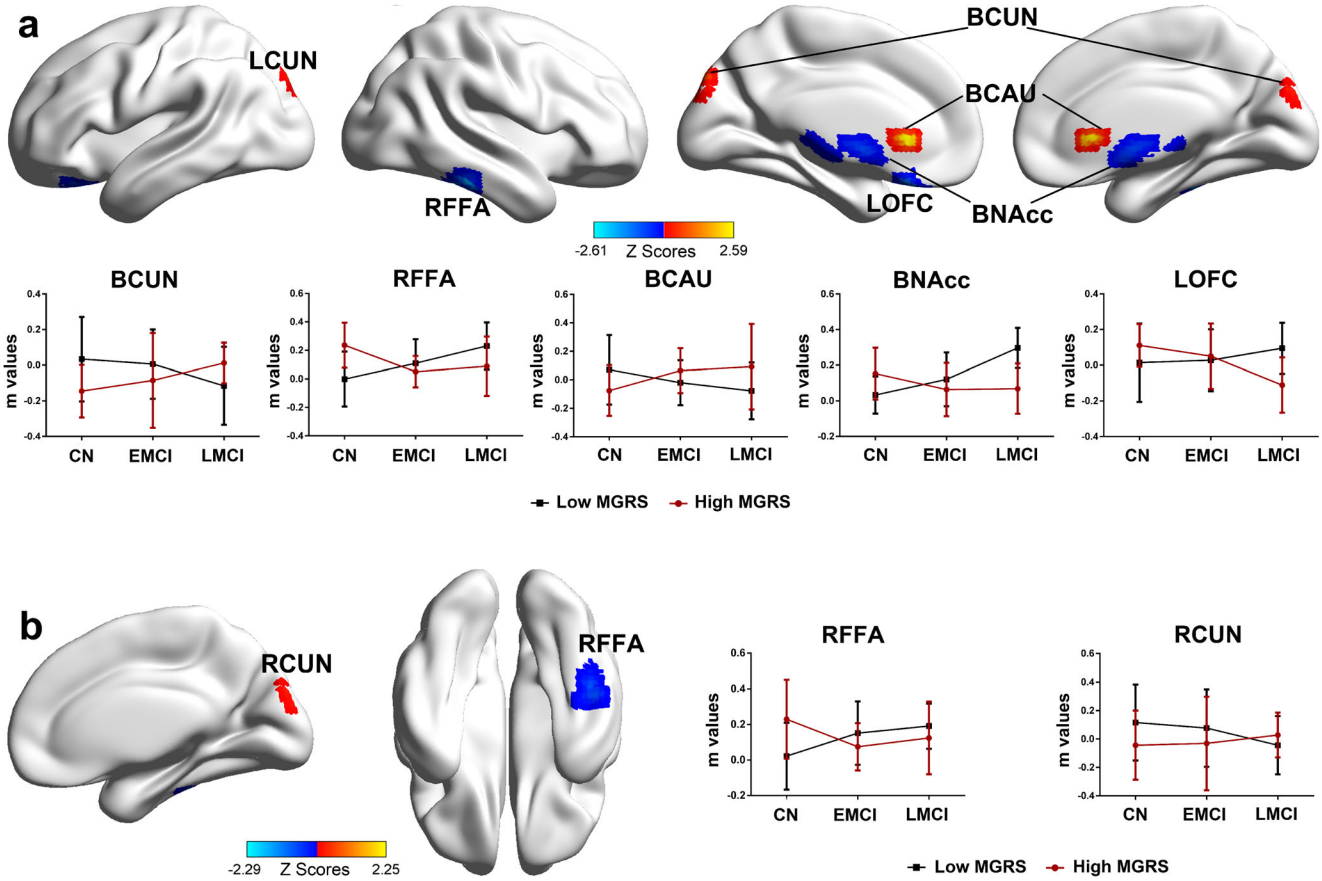

Fig. 4 Interactive effects produced by endocytosis-based MGRS and disease on HFC networks across all subjects. Brain regions with significant interactions between endocytosis-based MGRS and disease on HFC networks were shown in (**a**) (left HFC network) and (**b**) (right HFC network). The bright color indicated that the endocytosis-based MGRS and disease synergistically influenced the HFC network, and blue color indicated that the endocytosis-based MGRS and disease oppositely influenced the HFC network. Numerical representations of the significant interactive effects of endocytosis-based MGRS and disease status on the HFC were illustrated with line charts. Importantly, the trend for changed HFC strength was opposite in high endocytosis-based MGRS carriers compared to low endocytosis-based MGRS carriers across the prodromal stages of AD. Abbreviation: *CN* cognitive normal, *EMCI* early mild cognitive impairment, *LMCI* late mild cognitive impairment, *MGRS* multilocus genetic risk scores, *HFC* hippocampal functional connectivity, *LCUN* left cuneus, *RCUN* right cuneus, *BCUN* bilateral cuneus, *BCAU* bilateral caudate, *BNAcc* bilateral nucleus accumbens, *RFFA* right fusiform area, *LOFC* left orbitofrontal cortex

Brain regions with the main effects of the disease were primarily located in parietal and temporal lobes and NAcc, which have also been reported in other studies (Wang et al. 2006; Xie et al. 2013). The increased hippocampal connections with NAcc, pMTG, THA and decreased TPJ/IPC connectivity were found. TPJ and IPC, as the joint of the temporal-parietal-occipital cortex, were related to perception, recognition, and storage of memory materials (Jonides et al. 1998; Gusnard et al. 2001). Moreover, the hippocampus and NAcc showed significant atrophy in the AD and MCI patients compared to the CN group. The reductions in hippocampus and NAcc volumes were also associated with increased risk of MCI progression to AD. Furthermore, the loss of subcortical gray matter structures was related to the severity of cognitive impairment in AD and MCI patients (Yi et al. 2016; Nie et al. 2017). The increased HFC in baseline was followed by a longitudinal decrease in aMCI patients, suggesting that the initial observed enhanced connections was a compensatory process (Wang et al. 2011).

The endocytosis-based MGRS took effect on the intrinsic HFC network including LOFC, RFFA and BCUN. Specially, the endocytosis-based MGRS was positively correlated with LOFC and RFFA. Once OFC connections were disrupted, there could be a number of consequences of cognition, behavior, and emotion (Paulus et al. 2002). Neurofibrillary tangles (NFTs), as a key feature of AD pathology, were involved in the bilateral OFC and associated with agitation in AD patients (Tekin et al. 2001). FFA, as a cortical centre, showed synergistic activation when performing the facial matching task in normal ageing and MCI patients (Teipel et al. 2007; Tsao et al. 2008). Importantly, NFTs were found in the FFA region of normal ageing and MCI patients, and MCI patients produced more NFTs than normal control subjects (Guillozet et al. 2003). These studies suggested that structural and functional

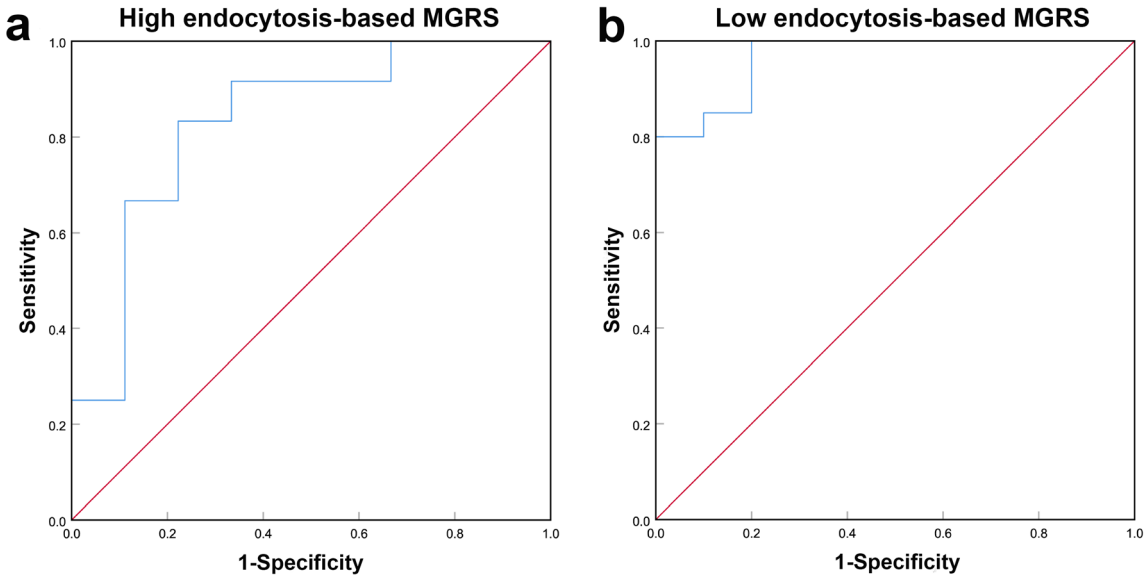

Fig. 5 Endocytosis-based MGRS-related HFC network and structure classified the EMCI and LMCI subjects. ROC curve, plot of the sensitivity versus (1-specificity) for distinguishing EMCI patients from LMCI patients. With an AUC of 0.833, stepwise discrimination analysis revealed the most discriminative features for classification involved the LHIP-RpMTG FC and LHIP volume in high endocytosis-based MGRS carriers (**a**). With an AUC of 0.965, the most discriminative features for classification involved the LHIP-RIPC/RTPJ, LHIP-RpMTG, RHIP-BCUN and RHIP-RFFA FCs in low endocytosis-based MGRS carriers (**b**). Abbreviation: *EMCI* early mild cognitive impairment, *LMCI* late mild cognitive impairment, *HFC* hippocampal functional connectivity, *ROC* receiver operating characteristic, *AUC* area under curve, *MGRS* multilocus genetic risk scores, *LHIP* left hippocampus, *RHIP* right hippocampus, *RpMTG* right posterior middle temporal gyrus, *RIPC/RTPJ* right inferior parietal cortex/right temporal-parietal junction, *BCUN* bilateral cuneus, *RFFA* right fusiform area

impairment of FFA may preferentially contribute to AD development, especially in visual cognition. Recently, The hypothesis of cascading network failure was proposed in the AD spectrum (Jones et al. 2016, 2017). This model suggested that the posterior default mode network (DMN) failed before the presence of measurable amyloid plaques, initiated the continuous cascade network and then shifted the processing burden to the other backbone regions throughout the AD spectrum. These backbone regions (many located in the frontal lobe) with high connectivity to the posterior DMN were associated with amyloid protein accumulation (Pasquini et al. 2017; Drzezga et al. 2011; Elman et al. 2016). The cascading failures network was characterized by local overloading, eventually leading to the entire DMN and other systems failing, which precedes structural and functional declines in the AD spectrum (Jones et al. 2016). In our study, we also found that the FC in the BCUN, as the hubs of posterior DMN, was decreased while the FC in the OFC was increased. Moreover, although the sample of the study was relatively small, we still found significant variability (5.8–11.4%) in the HFC network that was explained by the endocytosis-based MGRS. These findings supported the important role of polygenic effects of endocytosis pathway in the HFC network.

An interactive effect between diseases and the endocytosis-based MGRS was mainly located in the frontal-temporal-occipital and subcortical circuits. Prefrontal cortex-subcortical circuits has been linked with deficits in working memory, and consistently identified to be involved in the AD progression (Buckner et al. 2009; Smith 2002). Task-neuroimaging studies showed that subcortical regions were activated during working memory tasks in both primate and healthy human subjects. The CAU may also be associated with working memory and its volume was also negatively correlated with persistent errors in spatial working memory tasks (Hannan et al. 2010; Levitt et al. 2002). Intriguingly, the high and low endocytosis-based MGRS carriers produced approximately opposite FC changes with hippocampus to these target regions across the prodromal stages of AD, which might be ascribed to different neural mechanisms involved in AD progression. Specifically, the high endocytosis-based MGRS carriers in the EMCI group showed an increased FC, while the low endocytosis-based MGRS carriers showed decreased connectivity within BCUN and BCAU regions. Similar changes have been reported in MCI patients (Bai et al. 2009b). Moreover, our study further showed only *SORL1* risk score was positively correlated with RAVLT-immediate scores in MCI groups but the association failed to pass the multiple testing. It is worth noting that no correlation was detected with the combined risk scores in our study.

Some studies have tried to establish biomarkers to distinguish different stages of the AD spectrum. Appling fusion analysis to the DMN, neuropsychological scores and MRI volumes could possibly classify EMCI and LMCI patients (Pei et al. 2018; Goryawala et al. 2015). In this present study, we selected altered FCs and hippocampal volumes as independent variables for stepwise discrimination analysis in our

model to classify EMCI and LMCI patients. Interestingly, in the high endocytosis-based MGRS carriers, this composite model could possibly distinguish EMCI from LMCI patients with an accurately of 81.0% (sensitivity, 83.3%; specificity, 77.8%) by selecting LHIP-RpMTG connectivity and LHIP volume as discriminative features. While in the low endocytosis-based MGRS carriers, by taking LHIP-RTPJ, LHIP-RpMTG, RHIP-BCUN and RHIP-RFFA FCs as discriminative features, the model achieved the accuracy of 83.3% (sensitivity, 85.0%; specificity, 80.0%). Irrespective of the endocytosis-based MGRS, the classification model achieved the accuracy of 76.5% (sensitivity, 81.3%; specificity, 68.4%). This suggested the model based on the endocytic pathway yielded better classification performance in MCI patients. Our results indicated that in addition to the general cognitive function to be tested, for some patients with difficulty in evaluating or staging diagnosis, we could detect the endocytosis pathway genes and neuroimaging biomarkers from the HFC network in rs-fMRI. The integration of multiple biomarkers may help diagnose the prodromal stages of AD.

There are several limitations. First, due to the limited number of subjects available to us especially in the subgroup, we were only able to conduct a discovery study. Next, these endocytosis-based genes loci were restricted because of some SNPs missing in the ADNI database. A larger sample size (i.e., the number of SNPs) was needed to expand upon these preliminary findings. Third, we used the leave one out cross-validation method to verify the result. It is worth noting that significant neuroimaging indicators were selected from the same dataset as classification features, and this may limit the generability of our findings. In the future, it's better to validate our findings in a new dataset with the longitudinal study. Fourth, the brain function might be influenced by other pathway variants with regard to other AD hypotheses. Unbiased analysis of all pathways may provide a complete picture and would help to compare different pathways with endocytosis. Future studies focusing on complex pathways might provide more comprehensive exploratory information for better understanding mechanism underlying the AD pathophysiology.

Conclusion

In summary, we demonstrated that the endocytosis-based MGRS specifically contributes to the HFC network across the prodromal stages of AD. The trajectories of HFC between high and low endocytosis-based MGRS carriers are different from the normal to LMCI stage. Additionally, we propose that the combination of HFC strength and hippocampal volume might be useful as imaging biomarkers for classifying the stages of EMCI and LMCI. These findings provide new insight into the neural mechanisms that underlie prodromal stages of AD.

Acknowledgments Data collection and sharing for this project was funded by the Alzheimer's Disease.

Neuroimaging Initiative (ADNI) (National Institutes of Health Grant U01 AG024904) and DOD ADNI (Department of Defense award number W81XWH-12-2-0012). ADNI is funded by the National Institute on Aging, the National Institute of Biomedical Imaging and Bioengineering, and through generous contributions from the following: AbbVie, Alzheimer's Association; Alzheimer's Drug Discovery Foundation; Araclon Biotech; BioClinica, Inc.; Biogen; Bristol-Myers Squibb Company; CereSpir, Inc.; Cogstate; Eisai Inc.; Elan Pharmaceuticals, Inc.; Eli Lilly and Company; EuroImmun; F. Hoffmann-La Roche Ltd. and its affiliated company Genentech, Inc.; Fujirebio; GE Healthcare; IXICO Ltd.; Janssen Alzheimer Immunotherapy Research & Development, LLC.; Johnson & Johnson Pharmaceutical Research & Development LLC.; Lumosity; Lundbeck; Merck & Co., Inc.; Meso Scale Diagnostics, LLC.; NeuroRx Research; Neurotrack Technologies; Novartis Pharmaceuticals Corporation; Pfizer Inc.; Piramal Imaging; Servier; Takeda Pharmaceutical Company; and Transition Therapeutics. The Canadian Institutes of Health Research is providing funds to support ADNI clinical sites in Canada. Private sector contributions are facilitated by the Foundation for the National Institutes of Health (http://www.fnih.org). The grantee organization is the Northern California Institute for Research and Education, and the study is coordinated by the Alzheimer's Therapeutic Research Institute at the University of Southern California. ADNI data are disseminated by the Laboratory for Neuro Imaging at the University of Southern California.

Funding information This study was granted funding by the National Key Projects for Research and Development Program of China (2016YFC1305800, 2016YFC1305802, CMX), the National Natural Science Foundation of China (81,870,850, QGR; 81,671,256, CMX).

Compliance with ethical standards

Conflict of interest None reported.

Ethical approval All procedures performed in studies involving human participants were in accordance with the ethical standards of the institutional and/or national research committee and with the 1964 Helsinki declaration and its later amendments or comparable ethical standards.

Informed consent Written informed consent was obtained from all participants and/or authorized representatives and the study partners before any protocol-specific procedures were carried out in the ADNI study.

References

Ahmad, S., Bannister, C., van der Lee, S. J., Vojinovic, D., Adams, H. H. H., Ramirez, A., Escott-Price, V., Sims, R., Baker, E., Williams, J., Holmans, P., Vernooij, M. W., Ikram, M. A., Amin, N., & van Duijn, C. M. (2018). Disentangling the biological pathways involved in early features of Alzheimer's disease in the Rotterdam Study. *Alzheimers Dement, 14*(7), 848–857. https://doi.org/10.1016/j.jalz.2018.01.005.

Aisen, P. S., Petersen, R. C., Donohue, M. C., Gamst, A., Raman, R., Thomas, R. G., Walter, S., Trojanowski, J. Q., Shaw, L. M., Beckett, L. A., Jack CR Jr, Jagust, W., Toga, A. W., Saykin, A. J., Morris, J. C., Green, R. C., Weiner, M. W., & Alzheimer's Disease Neuroimaging Initiative. (2010). Clinical Core of the Alzheimer's disease neuroimaging initiative: Progress and plans. *Alzheimers Dement, 6*(3), 239–246. https://doi.org/10.1016/j.jalz.2010.03.006.

Alzheimer's disease facts and figures. (2016). *Alzheimers Dement, 12*(4), 459–509.

Atri, A. (2019). The Alzheimer's disease clinical spectrum: Diagnosis and management. *The Medical Clinics of North America, 103*(2), 263–293. https://doi.org/10.1016/j.mcna.2018.10.009.

Bai, F., Zhang, Z., Watson, D. R., Yu, H., Shi, Y., & Yuan, Y. (2009a). Abnormal white matter independent of hippocampal atrophy in amnestic type mild cognitive impairment. *Neuroscience Letters, 462*(2), 147–151. https://doi.org/10.1016/j.neulet.2009.07.009.

Bai, F., Zhang, Z., Watson, D. R., Yu, H., Shi, Y., Yuan, Y., Zang, Y., Zhu, C., & Qian, Y. (2009b). Abnormal functional connectivity of hippocampus during episodic memory retrieval processing network in amnestic mild cognitive impairment. *Biological Psychiatry, 65*(11), 951–958. https://doi.org/10.1016/j.biopsych.2008.10.017.

Bai, F., Xie, C., Watson, D. R., Shi, Y., Yuan, Y., Wang, Y., Yue, C., Teng, Y., Wu, D., & Zhang, Z. (2011). Aberrant hippocampal subregion networks associated with the classifications of aMCI subjects: A longitudinal resting-state study. *PLoS One, 6*(12), e29288. https://doi.org/10.1371/journal.pone.0029288.

Bai, F., Liao, W., Yue, C., Pu, M., Shi, Y., Yu, H., Yuan, Y., Geng, L., & Zhang, Z. (2016). Genetics pathway-based imaging approaches in Chinese Han population with Alzheimer's disease risk. *Brain Structure & Function, 221*(1), 433–446. https://doi.org/10.1007/s00429-014-0916-4.

Baig, S., Joseph, S. A., Tayler, H., Abraham, R., Owen, M. J., Williams, J., Kehoe, P. G., & Love, S. (2010). Distribution and expression of picalm in Alzheimer disease. *Journal of Neuropathology and Experimental Neurology, 69*(10), 1071–1077. https://doi.org/10.1097/NEN.0b013e3181f52e01.

Bertram, L., McQueen, M. B., Mullin, K., Blacker, D., & Tanzi, R. E. (2007). Systematic meta-analyses of Alzheimer disease genetic association studies: The AlzGene database. *Nature Genetics, 39*(1), 17–23. https://doi.org/10.1038/ng1934.

Biffi, A., Anderson, C. D., Desikan, R. S., Sabuncu, M., Cortellini, L., Schmansky, N., Salat, D., Rosand, J., & Alzheimer's Disease Neuroimaging Initiative (ADNI). (2010). Genetic variation and neuroimaging measures in Alzheimer disease. *Archives of Neurology, 67*(6), 677–685. https://doi.org/10.1001/archneurol.2010.108.

Bottino, C. M., Castro, C. C., Gomes, R. L., Buchpiguel, C. A., Marchetti, R. L., & Neto, M. R. (2002). Volumetric MRI measurements can differentiate Alzheimer's disease, mild cognitive impairment, and normal aging. *International Psychogeriatrics, 14*(1), 59–72.

Buckner, R. L., Sepulcre, J., Talukdar, T., Krienen, F. M., Liu, H., Hedden, T., Andrews-Hanna, J. R., Sperling, R. A., & Johnson, K. A. (2009). Cortical hubs revealed by intrinsic functional connectivity: Mapping, assessment of stability, and relation to Alzheimer's disease. *The Journal of Neuroscience, 29*(6), 1860–1873. https://doi.org/10.1523/jneurosci.5062-08.2009.

Carey, R. M., Balcz, B. A., Lopez-Coviella, I., & Slack, B. E. (2005). Inhibition of dynamin-dependent endocytosis increases shedding of the amyloid precursor protein ectodomain and reduces generation of amyloid beta protein. *BMC Cell Biology, 6*, 30. https://doi.org/10.1186/1471-2121-6-30.

Choy, R. W., Cheng, Z., & Schekman, R. (2012). Amyloid precursor protein (APP) traffics from the cell surface via endosomes for amyloid beta (Abeta) production in the trans-Golgi network. *Proceedings of the National Academy of Sciences of the United States of America, 109*(30), E2077–E2082. https://doi.org/10.1073/pnas.1208635109.

Cirrito, J. R., Kang, J. E., Lee, J., Stewart, F. R., Verges, D. K., Silverio, L. M., Bu, G., Mennerick, S., & Holtzman, D. M. (2008). Endocytosis is required for synaptic activity-dependent release of amyloid-beta in vivo. *Neuron, 58*(1), 42–51. https://doi.org/10.1016/j.neuron.2008.02.003.

Cormont, M., Meton, I., Mari, M., Monzo, P., Keslair, F., Gaskin, C., et al. (2003). CD2AP/CMS regulates endosome morphology and traffic to the degradative pathway through its interaction with Rab4 and c-Cbl. *Traffic, 4*(2), 97–112.

Cummings, J. (2018). The National Institute on Aging-Alzheimer's Association framework on Alzheimer's disease: Application to clinical trials. *Alzheimers Dement, 15*, 172–178. https://doi.org/10.1016/j.jalz.2018.05.006.

Dickerson, B. C., Goncharova, I., Sullivan, M. P., Forchetti, C., Wilson, R. S., Bennett, D. A., Beckett, L. A., & deToledo-Morrell, L. (2001). MRI-derived entorhinal and hippocampal atrophy in incipient and very mild Alzheimer's disease. *Neurobiology of Aging, 22*(5), 747–754.

Drzezga, A., Becker, J. A., Van Dijk, K. R., Sreenivasan, A., Talukdar, T., Sullivan, C., et al. (2011). Neuronal dysfunction and disconnection of cortical hubs in non-demented subjects with elevated amyloid burden. *Brain, 134*(Pt 6), 1635–1646. https://doi.org/10.1093/brain/awr066.

Dustin, M. L., Olszowy, M. W., Holdorf, A. D., Li, J., Bromley, S., Desai, N., Widder, P., Rosenberger, F., van der Merwe, P. A., Allen, P. M., & Shaw, A. S. (1998). A novel adaptor protein orchestrates receptor patterning and cytoskeletal polarity in T-cell contacts. *Cell, 94*(5), 667–677.

Elman, J. A., Madison, C. M., Baker, S. L., Vogel, J. W., Marks, S. M., Crowley, S., O'Neil, J. P., & Jagust, W. J. (2016). Effects of Beta-amyloid on resting state functional connectivity within and between networks reflect known patterns of regional vulnerability. *Cerebral Cortex, 26*(2), 695–707. https://doi.org/10.1093/cercor/bhu259.

Goryawala, M., Zhou, Q., Barker, W., Loewenstein, D. A., Duara, R., & Adjouadi, M. (2015). Inclusion of neuropsychological scores in atrophy models improves diagnostic classification of Alzheimer's disease and mild cognitive impairment. *Computational Intelligence and Neuroscience, 2015*, 865265–865214. https://doi.org/10.1155/2015/865265.

Guillozet, A. L., Weintraub, S., Mash, D. C., & Mesulam, M. M. (2003). Neurofibrillary tangles, amyloid, and memory in aging and mild cognitive impairment. *Archives of Neurology, 60*(5), 729–736. https://doi.org/10.1001/archneur.60.5.729.

Gusnard, D. A., Raichle, M. E., & Raichle, M. E. (2001). Searching for a baseline: Functional imaging and the resting human brain. *Nature Reviews. Neuroscience, 2*(10), 685–694. https://doi.org/10.1038/35094500.

Hannan, K. L., Wood, S. J., Yung, A. R., Velakoulis, D., Phillips, L. J., Soulsby, B., Berger, G., McGorry, P. D., & Pantelis, C. (2010). Caudate nucleus volume in individuals at ultra-high risk of psychosis: A cross-sectional magnetic resonance imaging study. *Psychiatry Research, 182*(3), 223–230. https://doi.org/10.1016/j.pscychresns.2010.02.006.

Hansen, C. G., & Nichols, B. J. (2009). Molecular mechanisms of clathrin-independent endocytosis. *Journal of Cell Science, 122*(Pt 11), 1713–1721. https://doi.org/10.1242/jcs.033951.

Hardy, J., & Selkoe, D. J. (2002). The amyloid hypothesis of Alzheimer's disease: Progress and problems on the road to therapeutics. *Science, 297*(5580), 353–356. https://doi.org/10.1126/science.1072994.

Harel, A., Wu, F., Mattson, M. P., Morris, C. M., & Yao, P. J. (2008). Evidence for CALM in directing VAMP2 trafficking. *Traffic, 9*(3), 417–429. https://doi.org/10.1111/j.1600-0854.2007.00694.x.

Harold, D., Abraham, R., Hollingworth, P., Sims, R., Gerrish, A., Hamshere, M. L., Pahwa, J. S., Moskvina, V., Dowzell, K., Williams, A., Jones, N., Thomas, C., Stretton, A., Morgan, A. R., Lovestone, S., Powell, J., Proitsi, P., Lupton, M. K., Brayne, C., Rubinsztein, D. C., Gill, M., Lawlor, B., Lynch, A., Morgan, K., Brown, K. S., Passmore, P. A., Craig, D., McGuinness, B., Todd, S., Holmes, C., Mann, D., Smith, A. D., Love, S., Kehoe, P. G., Hardy, J., Mead, S., Fox, N., Rossor, M., Collinge, J., Maier, W., Jessen, F., Schürmann, B., Heun, R., van den Bussche, H., Heuser, I.,

Kornhuber, J., Wiltfang, J., Dichgans, M., Frölich, L., Hampel, H., Hüll, M., Rujescu, D., Goate, A. M., Kauwe, J. S. K., Cruchaga, C., Nowotny, P., Morris, J. C., Mayo, K., Sleegers, K., Bettens, K., Engelborghs, S., de Deyn, P. P., van Broeckhoven, C., Livingston, G., Bass, N. J., Gurling, H., McQuillin, A., Gwilliam, R., Deloukas, P., al-Chalabi, A., Shaw, C. E., Tsolaki, M., Singleton, A. B., Guerreiro, R., Mühleisen, T. W., Nöthen, M. M., Moebus, S., Jöckel, K. H., Klopp, N., Wichmann, H. E., Carrasquillo, M. M., Pankratz, V. S., Younkin, S. G., Holmans, P. A., O'Donovan, M., Owen, M. J., & Williams, J. (2009). Genome-wide association study identifies variants at CLU and PICALM associated with Alzheimer's disease. *Nature Genetics, 41*(10), 1088–1093. https://doi.org/10.1038/ng.440.

Hollingworth, P., Harold, D., Sims, R., Gerrish, A., Lambert, J. C., Carrasquillo, M. M., et al. (2011). Common variants at ABCA7, MS4A6A/MS4A4E, EPHA1, CD33 and CD2AP are associated with Alzheimer's disease. *Nature Genetics, 43*(5), 429–435. https://doi.org/10.1038/ng.803.

Jessen, F., Wiese, B., Bachmann, C., Eifflaender-Gorfer, S., Haller, F., Kolsch, H., et al. (2010). Prediction of dementia by subjective memory impairment: Effects of severity and temporal association with cognitive impairment. *Archives of General Psychiatry, 67*(4), 414–422. https://doi.org/10.1001/archgenpsychiatry.2010.30.

Jones, D. T., Knopman, D. S., Gunter, J. L., Graff-Radford, J., Vemuri, P., Boeve, B. F., Petersen, R. C., Weiner, M. W., Jack CR Jr, & Alzheimer's Disease Neuroimaging Initiative. (2016). Cascading network failure across the Alzheimer's disease spectrum. *Brain, 139*(Pt 2), 547–562. https://doi.org/10.1093/brain/awv338.

Jones, D. T., Graff-Radford, J., Lowe, V. J., Wiste, H. J., Gunter, J. L., Senjem, M. L., Botha, H., Kantarci, K., Boeve, B. F., Knopman, D. S., Petersen, R. C., & Jack, C. R., Jr. (2017). Tau, amyloid, and cascading network failure across the Alzheimer's disease spectrum. *Cortex, 97*, 143–159. https://doi.org/10.1016/j.cortex.2017.09.018.

Jonides, J., Schumacher, E. H., Smith, E. E., Koeppe, R. A., Awh, E., Reuter-Lorenz, P. A., Marshuetz, C., & Willis, C. R. (1998). The role of parietal cortex in verbal working memory. *The Journal of Neuroscience, 18*(13), 5026–5034.

Kimura, N., & Yanagisawa, K. (2018). Traffic jam hypothesis: Relationship between endocytic dysfunction and Alzheimer's disease. *Neurochemistry International, 119*, 35–41. https://doi.org/10.1016/j.neuint.2017.07.002.

Koivunen, J., Scheinin, N., Virta, J. R., Aalto, S., Vahlberg, T., Nagren, K., Helin, S., Parkkola, R., Viitanen, M., & Rinne, J. O. (2011). Amyloid PET imaging in patients with mild cognitive impairment: A 2-year follow-up study. *Neurology, 76*(12), 1085–1090. https://doi.org/10.1212/WNL.0b013e318212015e.

Lambert, J. C., Ibrahim-Verbaas, C. A., Harold, D., Naj, A. C., Sims, R., Bellenguez, C., et al. (2013). Meta-analysis of 74,046 individuals identifies 11 new susceptibility loci for Alzheimer's disease. *Nature Genetics, 45*(12), 1452–1458. https://doi.org/10.1038/ng.2802.

Lee, J. H., Cheng, R., Honig, L. S., Vonsattel, J. P., Clark, L., & Mayeux, R. (2008). Association between genetic variants in SORL1 and autopsy-confirmed Alzheimer disease. *Neurology, 70*(11), 887–889. https://doi.org/10.1212/01.wnl.0000280581.39755.89.

Levitt, J. J., McCarley, R. W., Dickey, C. C., Voglmaier, M. M., Niznikiewicz, M. A., Seidman, L. J., Hirayasu, Y., Ciszewski, A. A., Kikinis, R., Jolesz, F. A., & Shenton, M. E. (2002). MRI study of caudate nucleus volume and its cognitive correlates in neuroleptic-naive patients with schizotypal personality disorder. *The American Journal of Psychiatry, 159*(7), 1190–1197. https://doi.org/10.1176/appi.ajp.159.7.1190.

Liu, X., Yue, C., Xu, Z., Shu, H., Pu, M., Yu, H., Shi, Y., Zhuang, L., Xu, X., & Zhang, Z. (2012). Association study of candidate gene polymorphisms with amnestic mild cognitive impairment in a Chinese population. *PLoS One, 7*(7), e41198. https://doi.org/10.1371/journal.pone.0041198.

Maldjian, J. A., Laurienti, P. J., Kraft, R. A., & Burdette, J. H. (2003). An automated method for neuroanatomic and cytoarchitectonic atlas-based interrogation of fMRI data sets. *Neuroimage, 19*(3), 1233–1239.

Mengel-From, J., Christensen, K., McGue, M., & Christiansen, L. (2011). Genetic variations in the CLU and PICALM genes are associated with cognitive function in the oldest old. *Neurobiology of Aging, 32*, (3), 554 e557–554 e511. https://doi.org/10.1016/j.neurobiolaging.2010.07.016.

Miaczynska, M., Pelkmans, L., & Zerial, M. (2004). Not just a sink: Endosomes in control of signal transduction. *Current Opinion in Cell Biology, 16*(4), 400–406. https://doi.org/10.1016/j.ceb.2004.06.005.

Mitchell, A. J. (2009). CSF phosphorylated tau in the diagnosis and prognosis of mild cognitive impairment and Alzheimer's disease: A meta-analysis of 51 studies. *Journal of Neurology, Neurosurgery, and Psychiatry, 80*(9), 966–975. https://doi.org/10.1136/jnnp.2008.167791.

Miyagawa, T., Ebinuma, I., Morohashi, Y., Hori, Y., Young Chang, M., Hattori, H., Maehara, T., Yokoshima, S., Fukuyama, T., Tsuji, S., Iwatsubo, T., Prendergast, G. C., & Tomita, T. (2016). BIN1 regulates BACE1 intracellular trafficking and amyloid-beta production. *Human Molecular Genetics, 25*(14), 2948–2958. https://doi.org/10.1093/hmg/ddw146.

Musiek, E. S., & Holtzman, D. M. (2015). Three dimensions of the amyloid hypothesis: Time, space and 'wingmen'. *Nature Neuroscience, 18*(6), 800–806. https://doi.org/10.1038/nn.4018.

Naj, A. C., Jun, G., Beecham, G. W., Wang, L. S., Vardarajan, B. N., Buros, J., Gallins, P. J., Buxbaum, J. D., Jarvik, G. P., Crane, P. K., Larson, E. B., Bird, T. D., Boeve, B. F., Graff-Radford, N. R., de Jager, P. L., Evans, D., Schneider, J. A., Carrasquillo, M. M., Ertekin-Taner, N., Younkin, S. G., Cruchaga, C., Kauwe, J. S. K., Nowotny, P., Kramer, P., Hardy, J., Huentelman, M. J., Myers, A. J., Barmada, M. M., Demirci, F. Y., Baldwin, C. T., Green, R. C., Rogaeva, E., George-Hyslop, P. S., Arnold, S. E., Barber, R., Beach, T., Bigio, E. H., Bowen, J. D., Boxer, A., Burke, J. R., Cairns, N. J., Carlson, C. S., Carney, R. M., Carroll, S. L., Chui, H. C., Clark, D. G., Corneveaux, J., Cotman, C. W., Cummings, J. L., DeCarli, C., DeKosky, S. T., Diaz-Arrastia, R., Dick, M., Dickson, D. W., Ellis, W. G., Faber, K. M., Fallon, K. B., Farlow, M. R., Ferris, S., Frosch, M. P., Galasko, D. R., Ganguli, M., Gearing, M., Geschwind, D. H., Ghetti, B., Gilbert, J. R., Gilman, S., Giordani, B., Glass, J. D., Growdon, J. H., Hamilton, R. L., Harrell, L. E., Head, E., Honig, L. S., Hulette, C. M., Hyman, B. T., Jicha, G. A., Jin, L. W., Johnson, N., Karlawish, J., Karydas, A., Kaye, J. A., Kim, R., Koo, E. H., Kowall, N. W., Lah, J. J., Levey, A. I., Lieberman, A. P., Lopez, O. L., Mack, W. J., Marson, D. C., Martiniuk, F., Mash, D. C., Masliah, E., McCormick, W. C., McCurry, S. M., McDavid, A. N., McKee, A. C., Mesulam, M., Miller, B. L., Miller, C. A., Miller, J. W., Parisi, J. E., Perl, D. P., Peskind, E., Petersen, R. C., Poon, W. W., Quinn, J. F., Rajbhandary, R. A., Raskind, M., Reisberg, B., Ringman, J. M., Roberson, E. D., Rosenberg, R. N., Sano, M., Schneider, L. S., Seeley, W., Shelanski, M. L., Slifer, M. A., Smith, C. D., Sonnen, J. A., Spina, S., Stern, R. A., Tanzi, R. E., Trojanowski, J. Q., Troncoso, J. C., van Deerlin, V. M., Vinters, H. V., Vonsattel, J. P., Weintraub, S., Welsh-Bohmer, K. A., Williamson, J., Woltjer, R. L., Cantwell, L. B., Dombroski, B. A., Beekly, D., Lunetta, K. L., Martin, E. R., Kamboh, M. I., Saykin, A. J., Reiman, E. M., Bennett, D. A., Morris, J. C., Montine, T. J., Goate, A. M., Blacker, D., Tsuang, D. W., Hakonarson, H., Kukull, W. A., Foroud, T. M., Haines, J. L., Mayeux, R., Pericak-Vance, M. A., Farrer, L. A., & Schellenberg, G. D. (2011). Common variants at MS4A4/MS4A6E, CD2AP, CD33 and EPHA1 are associated with late-onset Alzheimer's disease. *Nature Genetics, 43*(5), 436–441. https://doi.org/10.1038/ng.801.

Nie, X., Sun, Y., Wan, S., Zhao, H., Liu, R., Li, X., Wu, S., Nedelska, Z., Hort, J., Qing, Z., Xu, Y., & Zhang, B. (2017). Subregional structural alterations in hippocampus and nucleus Accumbens correlate with the clinical impairment in patients with Alzheimer's disease clinical Spectrum: Parallel combining volume and vertex-based approach. *Frontiers in Neurology, 8*, 399. https://doi.org/10.3389/fneur.2017.00399.

Pasquini, L., Benson, G., Grothe, M. J., Utz, L., Myers, N. E., Yakushev, I., et al. (2017). Individual correspondence of amyloid-beta and Intrinsic connectivity in the posterior default mode network across stages of Alzheimer's disease. *Journal of Alzheimer's Disease, 58*(3), 763–773. https://doi.org/10.3233/jad-170096.

Paulus, M. P., Hozack, N. E., Zauscher, B. E., Frank, L., Brown, G. G., Braff, D. L., & Schuckit, M. A. (2002). Behavioral and functional neuroimaging evidence for prefrontal dysfunction in methamphetamine-dependent subjects. *Neuropsychopharmacology, 26*(1), 53–63. https://doi.org/10.1016/s0893-133x(01)00334-7.

Pei, S., Guan, J., & Zhou, S. (2018). Classifying early and late mild cognitive impairment stages of Alzheimer's disease by fusing default mode networks extracted with multiple seeds. *BMC Bioinformatics, 19*(Suppl 19), 523. https://doi.org/10.1186/s12859-018-2528-0.

Pennanen, C., Kivipelto, M., Tuomainen, S., Hartikainen, P., Hanninen, T., Laakso, M. P., et al. (2004). Hippocampus and entorhinal cortex in mild cognitive impairment and early AD. *Neurobiology of Aging, 25*(3), 303–310. https://doi.org/10.1016/s0197-4580(03)00084-8.

Potkin, S. G., Guffanti, G., Lakatos, A., Turner, J. A., Kruggel, F., Fallon, J. H., Saykin, A. J., Orro, A., Lupoli, S., Salvi, E., Weiner, M., Macciardi, F., & for the Alzheimer's Disease Neuroimaging Initiative. (2009). Hippocampal atrophy as a quantitative trait in a genome-wide association study identifying novel susceptibility genes for Alzheimer's disease. *PLoS One, 4*(8), e6501. https://doi.org/10.1371/journal.pone.0006501.

Purcell, S., Neale, B., Todd-Brown, K., Thomas, L., Ferreira, M. A., Bender, D., et al. (2007). PLINK: A tool set for whole-genome association and population-based linkage analyses. *American Journal of Human Genetics, 81*(3), 559–575. https://doi.org/10.1086/519795.

Ramjaun, A. R., & McPherson, P. S. (1998). Multiple amphiphysin II splice variants display differential clathrin binding: Identification of two distinct clathrin-binding sites. *Journal of Neurochemistry, 70*(6), 2369–2376.

Ranasinghe, K. G., Hinkley, L. B., Beagle, A. J., Mizuiri, D., Dowling, A. F., Honma, S. M., Finucane, M. M., Scherling, C., Miller, B. L., Nagarajan, S. S., & Vossel, K. A. (2014). Regional functional connectivity predicts distinct cognitive impairments in Alzheimer's disease spectrum. *Neuroimage Clin, 5*, 385–395. https://doi.org/10.1016/j.nicl.2014.07.006.

Rodriguez-Rodriguez, E., Sanchez-Juan, P., Vazquez-Higuera, J. L., Mateo, I., Pozueta, A., Berciano, J., et al. (2013). Genetic risk score predicting accelerated progression from mild cognitive impairment to Alzheimer's disease. *Journal of Neural Transmission (Vienna), 120*(5), 807–812. https://doi.org/10.1007/s00702-012-0920-x.

Rogaeva, E., Meng, Y., Lee, J. H., Gu, Y., Kawarai, T., Zou, F., Katayama, T., Baldwin, C. T., Cheng, R., Hasegawa, H., Chen, F., Shibata, N., Lunetta, K. L., Pardossi-Piquard, R., Bohm, C., Wakutani, Y., Cupples, L. A., Cuenco, K. T., Green, R. C., Pinessi, L., Rainero, I., Sorbi, S., Bruni, A., Duara, R., Friedland, R. P., Inzelberg, R., Hampe, W., Bujo, H., Song, Y. Q., Andersen, O. M., Willnow, T. E., Graff-Radford, N., Petersen, R. C., Dickson, D., der, S. D., Fraser, P. E., Schmitt-Ulms, G., Younkin, S., Mayeux, R., Farrer, L. A., & St George-Hyslop, P. (2007). The neuronal sortilin-related receptor SORL1 is genetically associated with Alzheimer disease. *Nature Genetics, 39*(2), 168–177. https://doi.org/10.1038/ng1943.

Schmidt, V., Sporbert, A., Rohe, M., Reimer, T., Rehm, A., Andersen, O. M., & Willnow, T. E. (2007). SorLA/LR11 regulates processing of amyloid precursor protein via interaction with adaptors GGA and PACS-1. *The Journal of Biological Chemistry, 282*(45), 32956–32964. https://doi.org/10.1074/jbc.M705073200.

Scotland, P. B., Heath, J. L., Conway, A. E., Porter, N. B., Armstrong, M. B., Walker, J. A., Klebig, M. L., Lavau, C. P., & Wechsler, D. S. (2012). The PICALM protein plays a key role in iron homeostasis and cell proliferation. *PLoS One, 7*(8), e44252. https://doi.org/10.1371/journal.pone.0044252.

Seshadri, S., Fitzpatrick, A. L., Ikram, M. A., DeStefano, A. L., Gudnason, V., Boada, M., et al. (2010). Genome-wide analysis of genetic loci associated with Alzheimer disease. *JAMA, 303*(18), 1832–1840. https://doi.org/10.1001/jama.2010.574.

Smith, A. D. (2002). Imaging the progression of Alzheimer pathology through the brain. *Proceedings of the National Academy of Sciences of the United States of America, 99*(7), 4135–4137. https://doi.org/10.1073/pnas.082107399.

Smith, A. D., & Yaffe, K. (2014). Dementia (including Alzheimer's disease) can be prevented: Statement supported by international experts. *Journal of Alzheimer's Disease, 38*(4), 699–703. https://doi.org/10.3233/jad-132372.

Sohn, W. S., Yoo, K., Na, D. L., & Jeong, Y. (2014). Progressive changes in hippocampal resting-state connectivity across cognitive impairment: A cross-sectional study from normal to Alzheimer disease. *Alzheimer Disease and Associated Disorders, 28*(3), 239–246. https://doi.org/10.1097/wad.0000000000000027.

Sorkin, A., & Von Zastrow, M. (2002). Signal transduction and endocytosis: Close encounters of many kinds. *Nature Reviews. Molecular Cell Biology, 3*(8), 600–614. https://doi.org/10.1038/nrm883.

Sperling, R. A., Jack, C. R., Jr., & Aisen, P. S. (2011). Testing the right target and right drug at the right stage. *Science Translational Medicine, 3*(111), 111cm133. https://doi.org/10.1126/scitranslmed.3002609.

Sperling, R., Mormino, E., & Johnson, K. (2014). The evolution of preclinical Alzheimer's disease: Implications for prevention trials. *Neuron, 84*(3), 608–622. https://doi.org/10.1016/j.neuron.2014.10.038.

Spoelgen, R., von Arnim, C. A., Thomas, A. V., Peltan, I. D., Koker, M., Deng, A., et al. (2006). Interaction of the cytosolic domains of sorLA/LR11 with the amyloid precursor protein (APP) and beta-secretase beta-site APP-cleaving enzyme. *The Journal of Neuroscience, 26*(2), 418–428. https://doi.org/10.1523/jneurosci.3882-05.2006.

Su, F., Shu, H., Ye, Q., Wang, Z., Xie, C., Yuan, B., Zhang, Z., & Bai, F. (2017a). Brain insulin resistance deteriorates cognition by altering the topological features of brain networks. *Neuroimage Clin, 13*, 280–287. https://doi.org/10.1016/j.nicl.2016.12.009.

Su, F., Shu, H., Ye, Q., Xie, C., Yuan, B., Zhang, Z., & Bai, F. (2017b). Integration of multilocus genetic risk into the default mode network longitudinal trajectory during the Alzheimer's disease process. *Journal of Alzheimer's Disease, 56*(2), 491–507. https://doi.org/10.3233/jad-160787.

Teipel, S. J., Bokde, A. L., Born, C., Meindl, T., Reiser, M., Moller, H. J., et al. (2007). Morphological substrate of face matching in healthy ageing and mild cognitive impairment: A combined MRI-fMRI study. *Brain, 130*(Pt 7), 1745–1758. https://doi.org/10.1093/brain/awm117.

Tekin, S., Mega, M. S., Masterman, D. M., Chow, T., Garakian, J., Vinters, H. V., & Cummings, J. L. (2001). Orbitofrontal and anterior cingulate cortex neurofibrillary tangle burden is associated with agitation in Alzheimer disease. *Annals of Neurology, 49*(3), 355–361.

Tsao, D. Y., Schweers, N., Moeller, S., & Freiwald, W. A. (2008). Patches of face-selective cortex in the macaque frontal lobe. *Nature Neuroscience, 11*(8), 877–879. https://doi.org/10.1038/nn.2158.

Ubelmann, F., Burrinha, T., Salavessa, L., Gomes, R., Ferreira, C., Moreno, N., et al. (2017). Bin1 and CD2AP polarise the endocytic generation of beta-amyloid. *EMBO Reports, 18*(1), 102–122. https://doi.org/10.15252/embr.201642738.

Wang, L., Zang, Y., He, Y., Liang, M., Zhang, X., Tian, L., Wu, T., Jiang, T., & Li, K. (2006). Changes in hippocampal connectivity in the early stages of Alzheimer's disease: Evidence from resting state fMRI. *Neuroimage, 31*(2), 496–504. https://doi.org/10.1016/j.neuroimage.2005.12.033.

Wang, Z., Liang, P., Jia, X., Qi, Z., Yu, L., Yang, Y., Zhou, W., Lu, J., & Li, K. (2011). Baseline and longitudinal patterns of hippocampal connectivity in mild cognitive impairment: Evidence from resting state fMRI. *Journal of the Neurological Sciences, 309*(1–2), 79–85. https://doi.org/10.1016/j.jns.2011.07.017.

Weiler, M., Teixeira, C. V., Nogueira, M. H., de Campos, B. M., Damasceno, B. P., Cendes, F., et al. (2014). Differences and the relationship in default mode network intrinsic activity and functional connectivity in mild Alzheimer's disease and amnestic mild cognitive impairment. *Brain Connectivity, 4*(8), 567–574. https://doi.org/10.1089/brain.2014.0234.

Weiner, M. W., Aisen, P. S., Jack, C. R., Jr., Jagust, W. J., Trojanowski, J. Q., Shaw, L., Saykin, A. J., Morris, J. C., Cairns, N., Beckett, L. A., Toga, A., Green, R., Walter, S., Soares, H., Snyder, P., Siemers, E., Potter, W., Cole, P. E., & Schmidt, M. (2010). The Alzheimer's disease neuroimaging initiative: Progress report and future plans. *Alzheimers Dement, 6*(3), 202–211 e207. https://doi.org/10.1016/j.jalz.2010.03.007.

Wigge, P., & McMahon, H. T. (1998). The amphiphysin family of proteins and their role in endocytosis at the synapse. *Trends in Neurosciences, 21*(8), 339–344.

Williamson, J., Goldman, J., & Marder, K. S. (2009). Genetic aspects of Alzheimer disease. *Neurologist, 15*(2), 80–86. https://doi.org/10.1097/NRL.0b013e318187e76b.

Xiao, Q., Gil, S. C., Yan, P., Wang, Y., Han, S., Gonzales, E., Perez, R., Cirrito, J. R., & Lee, J. M. (2012). Role of phosphatidylinositol clathrin assembly lymphoid-myeloid leukemia (PICALM) in intracellular amyloid precursor protein (APP) processing and amyloid plaque pathogenesis. *The Journal of Biological Chemistry, 287*(25), 21279–21289. https://doi.org/10.1074/jbc.M111.338376.

Xie, C., Li, S. J., Shao, Y., Fu, L., Goveas, J., Ye, E., et al. (2011). Identification of hyperactive intrinsic amygdala network connectivity associated with impulsivity in abstinent heroin addicts. [Research Support, N.I.H., extramural Research Support, Non-U.S. Gov't]. *Behavioural Brain Research, 216*(2), 639–646. https://doi.org/10.1016/j.bbr.2010.09.004.

Xie, C., Li, W., Chen, G., Ward, B. D., Franczak, M. B., Jones, J. L., Antuono, P. G., Li, S. J., & Goveas, J. S. (2013). Late-life depression, mild cognitive impairment and hippocampal functional network architecture. *Neuroimage Clinical, 3*, 311–320. https://doi.org/10.1016/j.nicl.2013.09.002.

Xie, C., Bai, F., Yuan, B., Yu, H., Shi, Y., Yuan, Y., Wu, D., Zhang, Z. S., & Zhang, Z. J. (2015). Joint effects of gray matter atrophy and altered functional connectivity on cognitive deficits in amnestic mild cognitive impairment patients. *Psychological Medicine, 45*(9), 1799–1810. https://doi.org/10.1017/s0033291714002876.

Xu, J., Li, Q., Qin, W., Jun Li, M., Zhuo, C., Liu, H., Liu, F., Wang, J., Schumann, G., & Yu, C. (2018). Neurobiological substrates underlying the effect of genomic risk for depression on the conversion of amnestic mild cognitive impairment. *Brain, 141*(12), 3457–3471. https://doi.org/10.1093/brain/awy277.

Yajima, R., Tokutake, T., Koyama, A., Kasuga, K., Tezuka, T., Nishizawa, M., & Ikeuchi, T. (2015). ApoE-isoform-dependent cellular uptake of amyloid-beta is mediated by lipoprotein receptor LR11/SorLA. *Biochemical and Biophysical Research Communications, 456*(1), 482–488. https://doi.org/10.1016/j.bbrc.2014.11.111.

Ye, Q., Su, F., Shu, H., Gong, L., Xie, C., Zhang, Z., & Bai, F. (2016). The apolipoprotein E gene affects the three-year trajectories of compensatory neural processes in the left-lateralized hippocampal network. *Brain Imaging and Behavior, 11*, 1446–1458. https://doi.org/10.1007/s11682-016-9623-5.

Ye, Q., Su, F., Gong, L., Shu, H., Liao, W., Xie, C., Zhou, H., Zhang, Z., & Bai, F. (2017). Divergent roles of vascular burden and Neurodegeneration in the cognitive decline of geriatric depression patients and mild cognitive impairment patients. *Frontiers in Aging Neuroscience, 9*, 288. https://doi.org/10.3389/fnagi.2017.00288.

Yi, H. A., Moller, C., Dieleman, N., Bouwman, F. H., Barkhof, F., Scheltens, P., et al. (2016). Relation between subcortical grey matter atrophy and conversion from mild cognitive impairment to Alzheimer's disease. *Journal of Neurology, Neurosurgery, and Psychiatry, 87*(4), 425–432. https://doi.org/10.1136/jnnp-2014-309105.

Zhao, W., Wang, X., Yin, C., He, M., Li, S., & Han, Y. (2019). Trajectories of the hippocampal subfields atrophy in the Alzheimer's disease: A structural imaging study. *Frontiers in Neuroinformatics, 13*, 13. https://doi.org/10.3389/fninf.2019.00013.